SUPPLEMENTAL MATERIAL

Zaprinast enhanced Kir6.2/SUR1 channel activity in intact HEK293 cells in a concentration-dependent manner. To ascertain that the action of the cGMP-selective PDE inhibitor zaprinast is specific, we examined whether the effect of zaprinast on the single-channel activity of K_{ATP} channel in intact cells is concentration-dependent. Zaprinast was administered at 0.5, 5 or 50 μM by bath application in separate groups of cell-attached patches obtained from transfected HEK293 cells that expressed Kir6.2/SUR1 channels. We found that zaprinast elicited Kir6.2/SUR1 channel activation in a concentration-dependent fashion: there was no effect with 0.5 μM zaprinast (Supplemental Figs. 1A and 1D, open bar), whereas at 5 and 50 μM zaprinast increased the normalized *NPo* to 3.08 ± 0.57 (control as 1) (Supplemental Figs. 1B and 1D, hatched bar; $P < 0.05$) and 4.18 ± 0.23 (Supplemental Figs. 1C and 1D, filled bar; $P < 0.001$), respectively. These results indicate that zaprinast's stimulatory effect on Kir6.2/SUR1 channels results from its specific drug action. In the present study, 50 μM was chosen in all experiments involving the use of zaprinast.

Effects of zaprinast on the open- and closed-duration distributions of Kir6.2/SUR1 channels in intact cells were abolished by 5-HD, ROS scavengers and catalase. The open- and closed-duration distributions of the Kir6.2/SUR1 single-channel events in individual cell-attached patches could be best described by a sum of two open components and a sum of three closed components, respectively (Supplemental Fig. 2A, upper panel; from a SH-SY5Y cell). Effects of activation of PKG by zaprinast on the relative distributions of Kir6.2/SUR1 channel open and closed states (conformations) of different dwelling times were described in the main text (Fig. 3A; same data shown in Supplemental Fig. 2A for comparison purpose). There was no change in individual open time constants, but the channel exhibited a tendency to open into the longer open state more frequently in comparison with its opening pattern under the control condition (Supplemental Fig. 2A, Open). The number of closed components that best described the closed-duration distributions of Kir6.2/SUR1 channels during zaprinast application was the

same as in the control (three closed components); however, the time constant and relative area of the longest closed state was decreased during zaprinast treatment (Supplemental Fig. 2A, Closed). The change in the closed time constant, plus a tendency for the channel to reduce the occurrence of longest closures while to increase the occurrence of the long open state, largely accounted for a reduction in the normalized mean closed duration and an increase in the normalized corrected mean open duration by zaprinast (see Table 1 in main text, Zaprinast). By contrast, effects of zaprinast on the open- and closed-duration distributions of Kir6.2/SUR1 channels were prevented by the mitoK_{ATP} channel inhibitor 5-HD, the ROS scavenger MPG, and the H_2O_2-decomposing enzyme catalase (Supplemental Fig. 2B-D, lower vs. upper panels; representative cell-attached patches from SH-SY5Y cells). Our results thus indicate that PKG modified the open- and closed-duration distributions of Kir6.2/SUR1 channels through a 5-HD-sensitive factor- and ROS-dependent mechanism, thereby achieving channel stimulation.

Effects of NO/PKG/ROS signaling on the gating properties of neuronal-type K_{ATP} channels. Kinetically, the enhancement of Kir6.2/SUR1 single-channel currents by PKG activation (Figs. 1 and 2) was due to changes in the single-channel open and closed properties, including increases in normalized *NPo*, opening frequency and the corrected mean open duration, plus reduction in mean closed duration, without altering the single-channel conductance (Table 1). PKG activation altered the mean open and closed durations of the K_{ATP} channel by shifting the relative distribution of open and closed states (Fig. 4A). Similar changes in the aforementioned single-channel properties were reproduced by application of the NO donor NOC-18 as well as exogenous H_2O_2 elicited of Kir6.2/SUR1 channels in intact cells (Fig. 4B,C; Tables 2 and 3). Moreover, the kinetic effects of PKG activation and NO induction on neuronal-type K_{ATP} channels were abolished or attenuated by the mitoK_{ATP} channel inhibitor 5-HD, the ROS scavenger MPG, or the H_2O_2-decomposin enzyme catalase (Tables 1, 2 and 3; Supplemental Fig. 2). These results thus provide a kinetic interpretation of the roles of 5-HD-sensitive factor(s) and ROS in mediating neuronal K_{ATP} channel stimulation induced by NO and PKG. On the other hand, the presence of 5-HD did not affect the effects of exogenous H_2O_2 on

either increasing opening frequency and *NPo* or shortening the closed duration of Kir6.2/SUR1 channels in intact HEK293 cells (Table 3), which supports that the stimulatory action of H_2O_2 on neuronal K_{ATP} channels is not mediated by opening mitoK_{ATP} channels or activating the 5-HD sensitive protein(s), and allows us to propose the 5-HD sensitive protein(s) as an upstream signal of H_2O_2/ROS for mediating PKG-induced K_{ATP} channel stimulation. We thus suggest that activation of the NO/PKG/5-HD-sensitive factor/ROS signaling cascade positively modulates the function of neuronal K_{ATP} channels by destabilizing the closed states and increasing the frequency of closed-to-open transitions of the channels.

Measurement of intracellular ROS generation. In addition to direct measurements of the single-channel currents of K_{ATP} channels, we also investigated whether PKG activation causes detectable changes in the intracellular ROS level, by employing scanning confocal microscopy and the use of reduced Mito Tracker Red (500 nM; CM-H_2TMRos; Molecular Probes of Invitrogen, Carlsbad, CA), a chemically reactive reduced rosamine. CM-H_2TMRos does not fluoresce until it enters an actively respiring cell, where it is oxidized predominately by reaction involving H_2O_2; the positive charge acquired on oxidation by intracellular ROS made the probe covalently bind to mitochondrial proteins, producing a permanent organelle-specific stain (1). Intracellular ROS levels were monitored before and during zaprinast (50 μM) treatment, with vehicle (Hank's Balanced Salt Solution; HBSS) and H_2O_2 (1 mM) applied to separate groups of coverslips serving as negative and positive controls, respectively. In contrast to 1 mM H_2O_2, which markedly increased the intracellular ROS signal (Supplemental Fig. 3D), we found that the PKG activator zaprinast (Supplemental Fig. 3B), the vehicle group (Supplemental Fig. 3A) and 0.01 mM H_2O_2 (Supplemental Fig. 3C), all failed to elicit a detectable increase in intracellular ROS intensity (Supplemental Fig. 3E). However, it should be pointed out that 0.01 mM H_2O_2, like zaprinast (Figs. 1D,E,F and 2C,D,E; Table 1), was capable of enhancing the single-channel activity of Kir6.2/SUR1 K_{ATP} channels in intact HEK293 cells (Supplemental Fig. 3F; a representative patch). Therefore, it is possible that ROS generation occurring during PKG activation may be modest and thereby falls below the detection threshold

of the imaging technique in intact cells. Although ROS generation may be low during PKG activation, our single-channel data acquired in the absence and presence of ROS-reducing reagents and enzymes (Figs. 1, 2 and 3; Tables 1 and 2) strongly suggest that PKG stimulation of neuronal-type K_{ATP} channels depends on intracellular ROS generation. In fact, a small (rather than robust) increase in the intracellular ROS level during PKG activation, as implied here, is more compatible with a role of ROS in cell signaling downstream of PKG activation to open neuronal K_{ATP} channels.

PKG stimulation of neuronal-type K_{ATP} channels was not affected by molecular disruption of the MgADP sensitivity of the channel or metabolic inhibition of the cell. We showed that stimulation of the neuronal-type K_{ATP} channels by PKG activation (Figs. 1, 2 and 4A; Table 1), NO induction (Figs. 3 and 4B; Table 2) or H_2O_2 (Figs. 4C and 5A,B; Table 3) was associated with changes in the open and closed properties of the channel, which suggests that the altered channel properties may form the basis of PKG modulation of the channel. To ascertain that the stimulatory effect of PKG/ROS signaling on K_{ATP} channels is not secondary to changes in cellular metabolic states, we examined the effect of PKG activation on mutant K_{ATP} channels that exhibit a loss of MgADP sensitivity. The missense G1479R mutation in the second nucleotide binding fold of SUR1, a molecular defect associated with persistent hyperinsulinemic hypoglycemia of infancy, renders the K_{ATP} channel MgADP-insensitive while retaining normal ATP sensitivity (3,4). If PKG stimulation of the K_{ATP} channel depends on changes in the intracellular ADP level, the mutant Kir6.2/SUR1G1479R channel in intact cells would not be stimulated by PKG activation. Interestingly, we found that the PKG activator zaprinast (50 μM) stimulated both wild-type Kir6.2/SUR1 and mutant Kir6.2/SUR1G1479R channels in cell-attached patches obtained from transfected HEK293 cells, and the effects of zaprinast on the open and closed properties of these two channel constructs were indistinguishable (Supplemental Table 1). These findings thus indicate that the stimulation of neuronal K_{ATP} channels by PKG in intact cells did not result from changes in intracellular MgADP level or the MgADP sensitivity of the channel. On the other hand, our data on the Kir6.2FL4A channel (see Fig. 5C,E; Table 3,

Kir6.2FL4A) reveal that PKG and H_2O_2 were unable to enhance the currents of tetrameric channels formed solely by the pre-forming Kir6.2 subunit (which renders the ATP sensitivity to the channel). In addition, we found that PKG stimulation of the Kir6.2/SUR1 channels in intact cells was not affected in cells subjected to metabolic inhibition by sodium azide (data not shown). Hence, it is unlikely that PKG/ROS stimulation of neuronal K_{ATP} channels is caused by reduced cellular ATP production, either. Based on our findings (see Fig. 4; Tables 1-4), we suggest that changes in the intrinsic open and closed properties of the K_{ATP} channel may account for the stimulatory action of NO/PKG/ROS signaling on the channel.

REFERENCES

1. **Degli Esposti M.** Measuring mitochondrial reactive oxygen species. *Methods* 26(4): 335-340, 2002.

2. **Forbes RA, Steenbergen C, Murphy E.** Diazoxide-induced cardioprotection requires signaling through a redox-sensitive mechanism. *Circ Res* 88(8):802-809, 2001.

3. **Nichols CG, Shyng SL, Nestorowicz A, Glaser B, Clement JP 4th, Gonzalez G, Aguilar-Bryan L, Permutt MA, Bryan J.** Adenosine diphosphate as an intracellular regulator of insulin secretion. *Science* 272(5269):1785-7, 1996.

4. **Shyng S-L, Ferrigni T, Nichols CG.** Regulation of K_{ATP} channel activity by diazoxide and MgADP: distinct functions of the two nucleotide binding folds of the sulphonylurea receptor. *J Gen Physiol* 110: 643-654, 1997.

Supplemental Fig. 1. The cGMP-selective PDE inhibitor zaprinast concentration-dependently enhances Kir6.2/SUR1 channel activity in intact cells. Recombinant Kir6.2/SUR1 channels were expressed in HEK293 cells by transient transfection. Cell-attached patch recordings were performed as described in Fig. 1 of the main text. (**A-C**) Single-channel current traces of the Kir6.2/SUR1 channel obtained from representative cell-attached patches prior to (upper panel) and during (lower panel) application of the cGMP-specific PDE inhibitor zaprinast at increasing concentrations from 0.5 (**A**), 5 (**B**), to 50 (**C**) μM. Downward deflections represent openings from closed states. Marked segments of raw current traces (with horizontal lines atop) are shown in successive traces at increasing temporal resolution. The horizontal scale bars represent 1 s, 300 ms and 100 ms for traces from top to bottom in each panel, and the vertical scale bar represents 4 pA. (**D**) Normalized *NPo* of Kir6.2/SUR1 channels obtained during application of three concentrations of zaprinast in individual groups of cell-attached patches. *NPo* values were normalized to the corresponding control (taken as 1) obtained prior to drug application in individual patches. Dashed line indicates the control level. Data are presented as mean ± SEM of 4-6 patches. Significance levels are: *, $P < 0.05$; ***, $P < 0.001$ (two-tailed one-sample *t* tests within individual groups).

Supplemental Fig. 2. Effects of zaprinast on the open- and closed-duration distributions of Kir6.2/SUR1 channels in the absence and presence of 5-HD, ROS scavengers and catalase. Representative cell-attached patches were obtained from transfected SH-SY5Y cell expressing Kir6.2/SUR1 channels. Frequency histograms of duration distributions fitted from events obtained prior to (upper panel) and during (lower panel) application of the cGMP-specific PDE inhibitor zaprinast (50 μM) alone (**A**), or zparinast (50 μM) together with each of the following: the mitoK_{ATP} channel inhibitor 5-HD (100 μM) (**B**), the membrane-permeable ROS scavenger MPG (500 μM) (**C**), or catalase, a H_2O_2-decomposing enzyme (500 U/ml) (**D**). Open-duration distributions are displayed at left (*Open*) and closed-duration distributions at right (*Closed*), respectively, for each patch. Duration histograms were constructed as described in Materials and Methods. The frequency histograms shown in **A** are the same as presented in Fig. 4A of the main text, which are included here for comparison purpose.

Supplemental Fig. 3. PKG activation does not elicit a detectable increase in intracellular ROS levels. (**A-D**) Confocal images of HEK293 cells before (left column) and during (right column) treatment of a Hank's balanced salt solution (HBSS; vehicle) (**A**), zaprinast (**B**), 0.01 mM H_2O_2 (**C**), and 1 mM H_2O_2 (**D**). Cells were loaded with the ROS indicator CM-H_2TMRos (500 nM) for 20 min at room temperature. Zaprinast (50 μM) was applied by bath perfusion to activate PKG, while HBSS and H_2O_2 (1 mM) were applied to separate coverslips as negative and positive controls, respectively. A lower concentration of H_2O_2 (0.01 mM) was also included. Intracellular ROS levels, probed by oxidized CM-H_2TMRos (which fluoresces red), were monitored before and after drug treatment. Fluorescence images were recorded using an LSM 510 laser scanning confocal imaging system (Carl Zeiss, Inc., Jena, Germany) via a 40×/1.3 n.a. oil immersion objective. A 543 nm excitation light and 560 nm LP emission filter were used to acquire oxidized CM-H_2TMRos fluorescence. Image acquisition settings were identical for different experiments. Four to eight regions of interest (ROIs) were randomly selected from each coverslip, and single optical planes of 9 μm in depth were obtained for at 30-sec intervals for at least 30 min. Each experiment was repeated in three to six coverslips. (**E**) Changes in the rate of fluorescence increase in CM-H_2TMRos-loaded cells in response to the addition of HBSS, zaprinast and H_2O_2. Image analysis was performed off-line using LSM510 (Carl Zeiss) image analysis software (v. 4.2). For statistical analysis, rate of changes (i.e., "slopes") of the fluorescence intensity of individual ROIs under the control and treatment conditions was respectively calculated, and the differences of slopes were examined within (one-sample *t* test; control as 0) and between (one-way ANOVA followed by Dunnett's multiple comparison tests) groups. Data are presented as the rate of increase in fluorescence after treatment minus the initial (pretreatment) rate of increase in fluorescence (2) in mean ± SEM of 24-33 ROIs from individual groups. Significance level is: ****, $P < 0.0001$. (**F**) Single-channel current traces of the Kir6.2/SUR1 channel in a representative cell-attached patch obtained from a transfected HEK293 cell prior to (upper panel) and during (lower panel) bath application of 0.01 mM H_2O_2. The horizontal scale bar represents 1 s, and the vertical scale bar represents 4 pA. Although 0.01

mM H_2O_2 was unable to induce a detectable increase in the intracellular ROS level probed by oxidized CM-H_2TMRos, it effectively increased the Kir6.2/SUR1 channel currents. Considering this result, plus the functional data supportive of ROS involvement in PKG signaling (Figs. 1D-F, 2C-E, 3D-F, and 7; Tables 1-3), we suggest that the PKG activation may only induce generation of ROS at a modest quantity which falls undetected by the ROS dye measurement method in intact cells; however, the small change in ROS appears to be sufficient to mediate stimulation of neuronal K_{ATP} channels by NO and PKG.

Supplemental Table 1. *Effects of molecular disruption of the MgADP sensitivity of the K_{ATP} channel on PKG-induced changes in the normalized single-channel open and closed properties of the channel expressed in intact HEK293 cells*

Properties	Kir6.2/fSUR1	Kir6.2/fSUR1G1479R
Open probability	$3.16 \pm 0.70^{*}$	$4.77 \pm 1.08^{**}$
Opening frequency	$2.81 \pm 0.40^{*}$	$3.68 \pm 0.60^{**}$
Mean open duration	1.20 ± 0.27	1.23 ± 0.15
Mean closed duration	$0.36 \pm 0.11^{**}$	$0.34 \pm 0.05^{****}$
Number of patches	5	9

Single-channel recordings of Kir6.2/fSUR1 and Kir6.2/fSUR1G1479 channels expressed in transfected HEK293 cells were performed at –60 mV in symmetrical 140-mM K^+ solutions in the cell-attached patch configuration. Zaprinast (50 μM) was applied by bath perfusion using a pressure-driven system. The single-channel properties were obtained as described in Materials and Methods. All values were normalized to the corresponding controls obtained in individual patches prior to drug application (control taken as 1), averaged and are presented as mean ± SEM. Significance levels are: *, P <0.05; **, P <0.01; ****, P < 0.0001 (two-tailed one-sample *t* tests).

Suppl. Figure 1

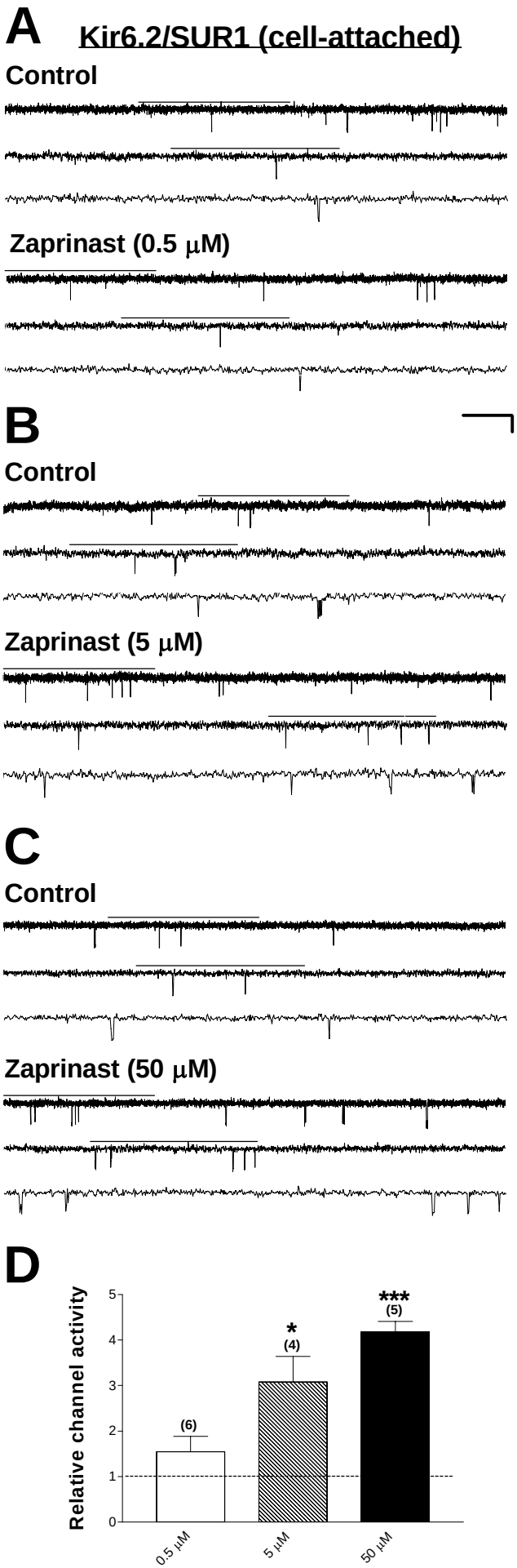

Suppl. Figure 2

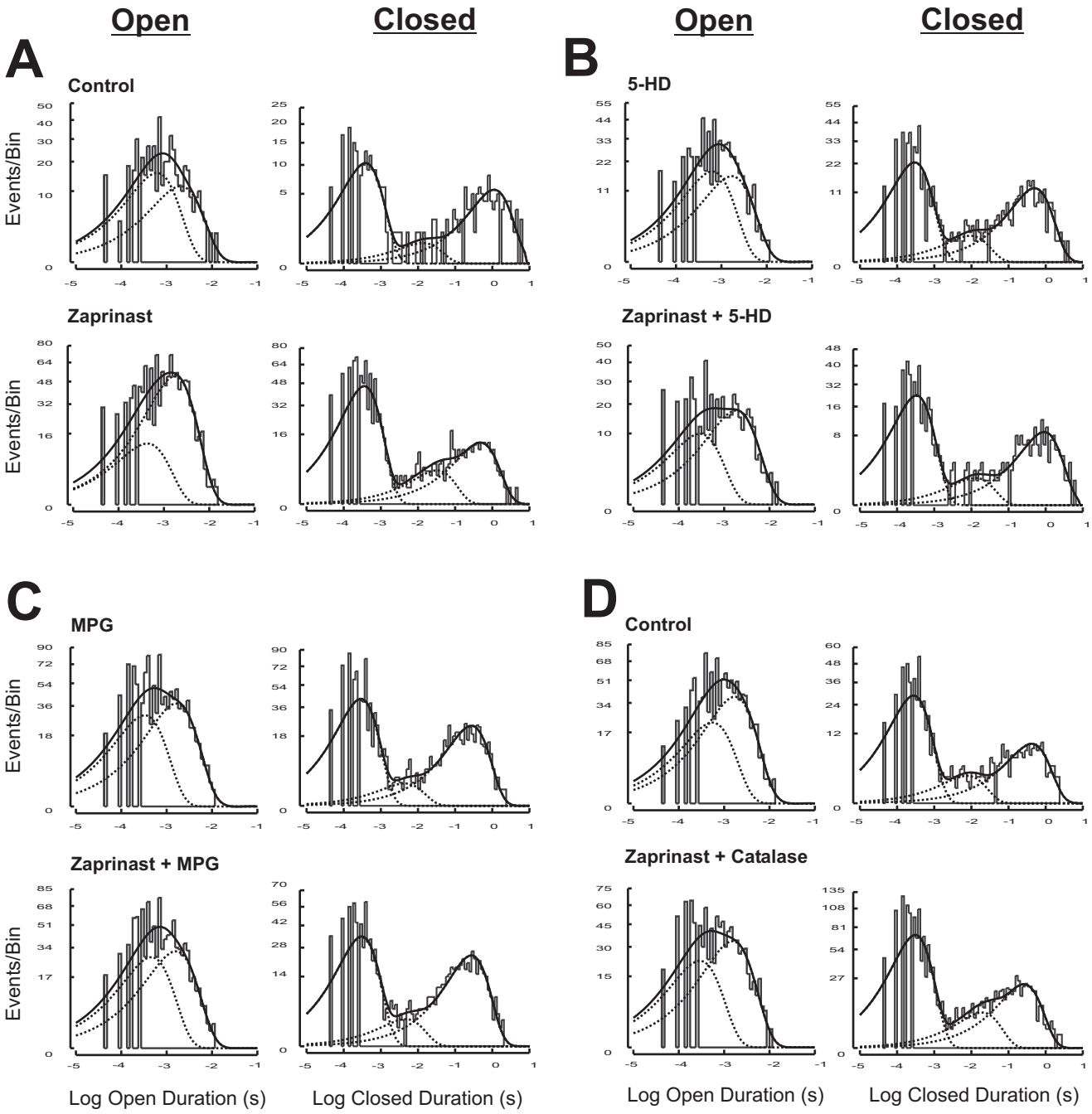

Suppl. Figure 3